Waves and generalised continua in bone biomechanics and tissue engineering

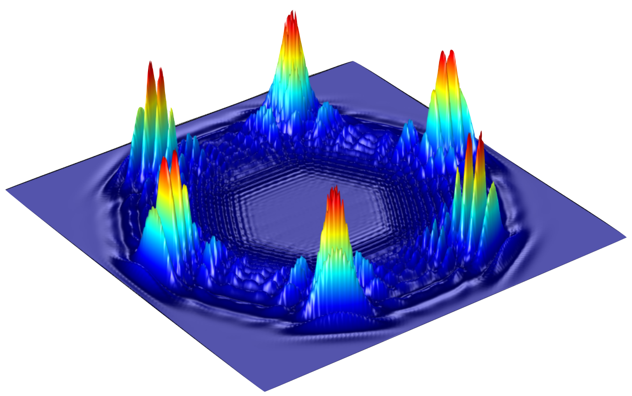

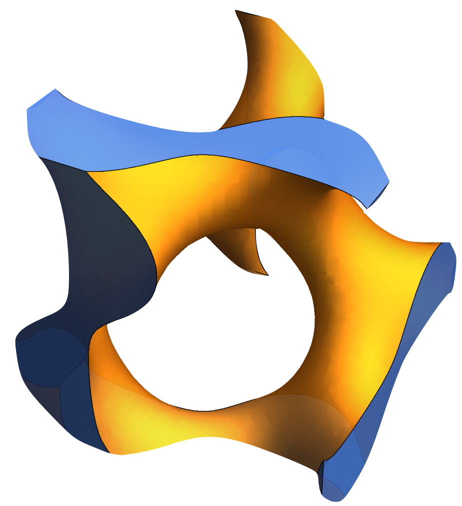

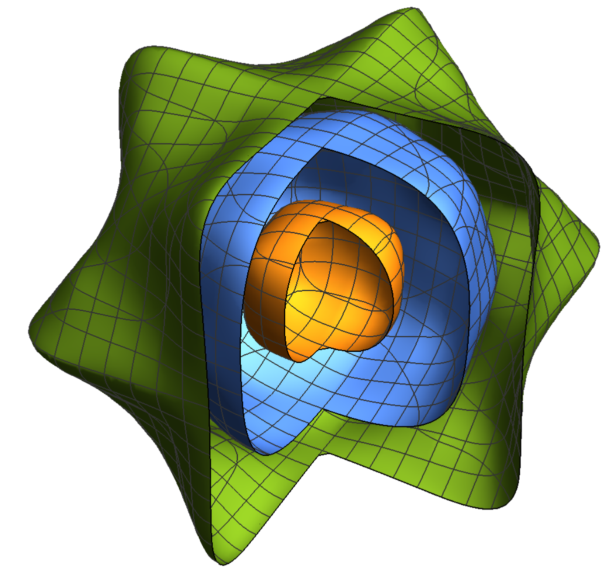

Giuseppe Rosi

Multi-Scale Modelling and Simulation Laboratory
Laboratoire Modélisation et Simulation Multi-Echelle
Université Paris-Est CNRS UMR 8208

Coss&Vita

Workshop ELADYN
18-11-2019

Waves and ultrasounds

Elastic waves are currently used in several fields, such as non-destructive evaluation, characterisation, and diagnostics.

Principle : when a wave propagates inside a material, it carries information about the mechanical properties of the material itself.

Information is extracted solving an **inverse problem.**

Main strategies:

Time of flight, amplitude

Bulk propagation and reflections at boundaries (imaging)

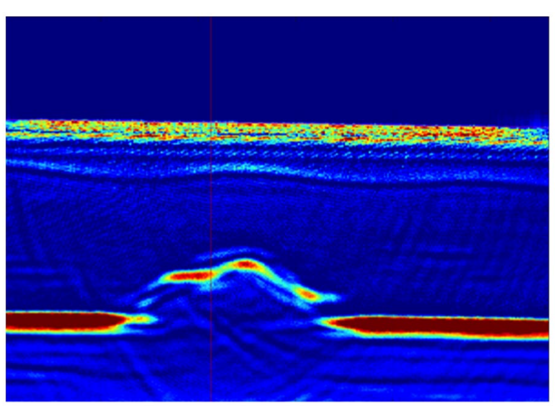

Dispersion

Guided propagation (surface waves, Lamb waves)

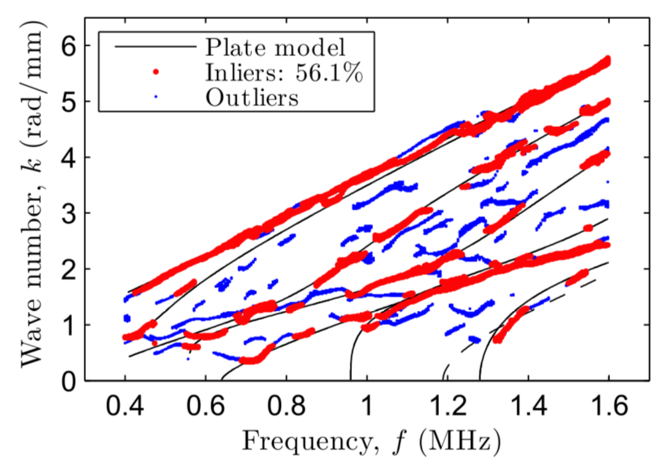

Bochud, N. et al (2017). Predicting bone strength with ultrasonic guided waves. Scientific Reports, 7, 43628

Multi scale tissue modelling and characterisation

Organ scale

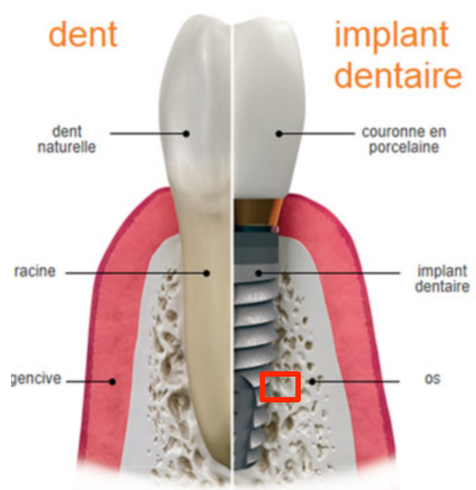

Dental implant

Orthopaedic implant


Bone scaffold implant

Tissue scale

Micro scale

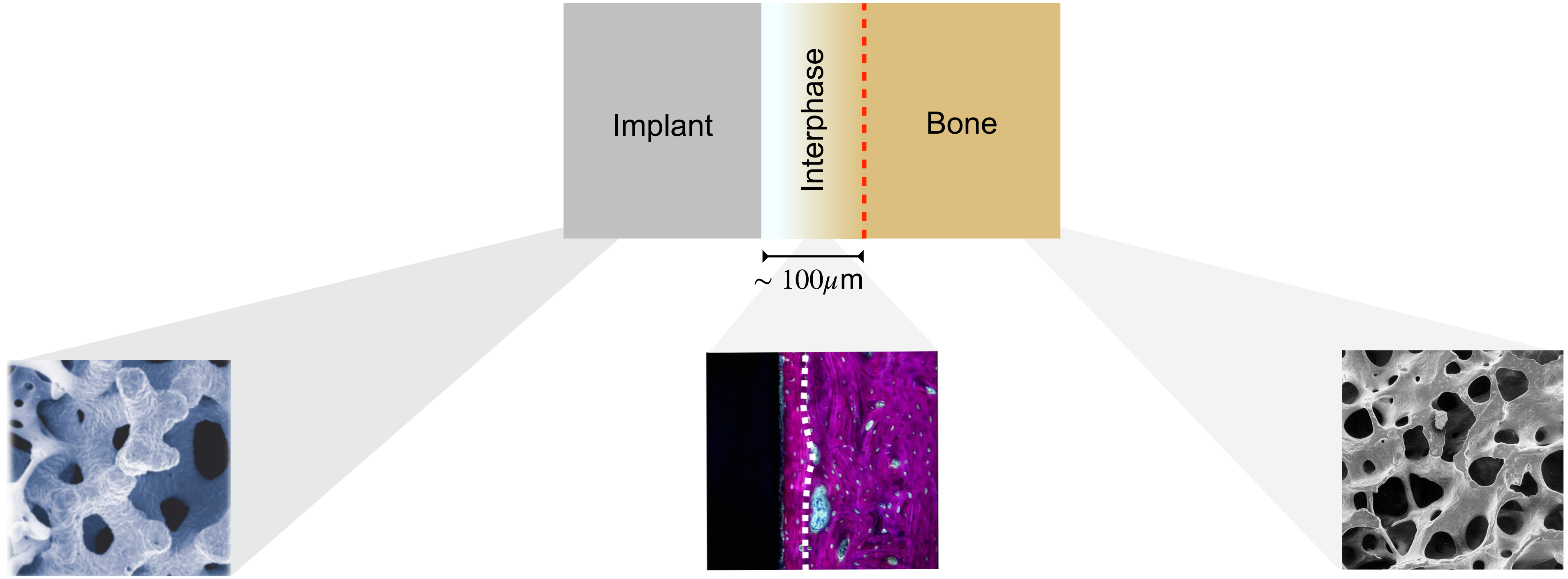

Implant

- Microstructure
- Porosity
- Tissue engineering
- Multiple optimisation constraints
- Boundary conditions

Interphase

- Heterogeneity
- Mesh refinement
- Computational costs
- Evolving conditions (osteointegration)
- Boundary conditions

Bone

- Microstructure
- Heterogeneity
- Porosity
- Remodelling
- Boundary conditions

Architectured implants and tissue engineering

Optimisation of the mechanical properties or reduction of stress shielding

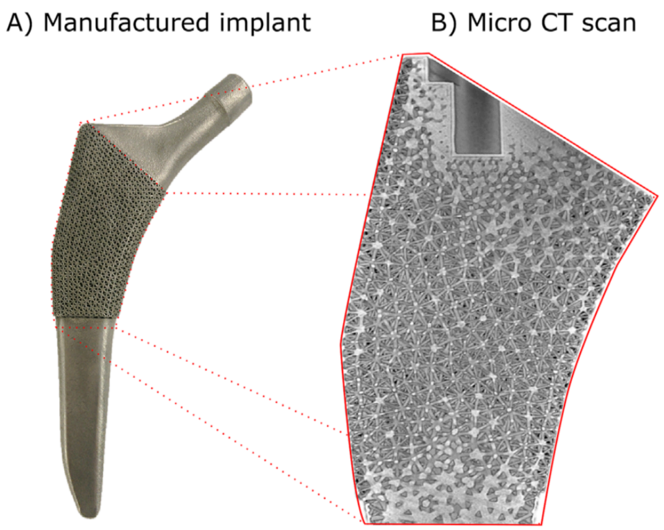

Fully porous implant
(Titanium)

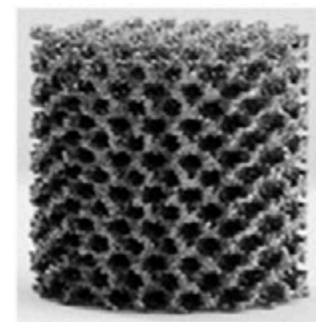

Gyroid scaffold
(Titanium)

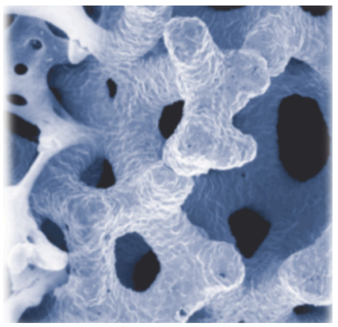

Zimmer's
Trabecular metal™
(Tantalum)

Modelling and simulation challenges and objectives:

- Take into account microstructure effects
- Describe complex boundary conditions
- Cost (or utility) functions to be used in optimisation

Yánez, A. et al. (2018). Gyroid porous titanium structures: A versatile solution to be used as scaffolds in bone defect reconstruction. Materials & Design, 140, 21–29.

Arabnejad, S. et al. (2017). Fully porous 3D printed titanium femoral stem to reduce stress-shielding following total hip arthroplasty. Journal of Orthopaedic Research, 35(8), 1774–1783.

Nature loves regular microstructures!

Hexagonal honeycomb maximise the area vs the perimeter (for regular tilings) and isotropic mechanical properties

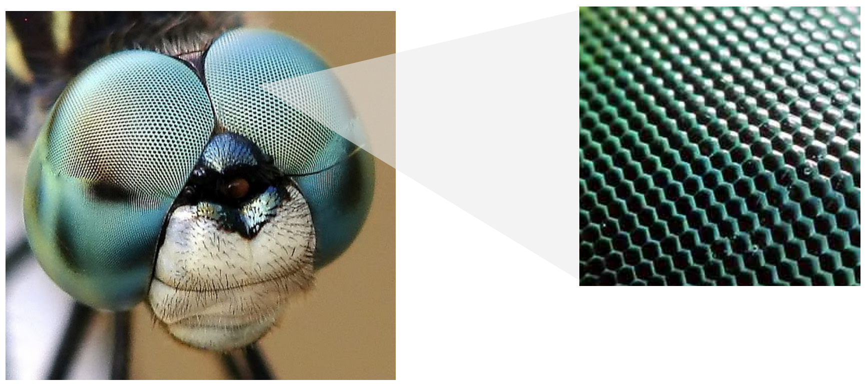

Gyroids are a minimal surfaces (obtained e.g. as assembly of co-block polymers) and are used as photonic crystals

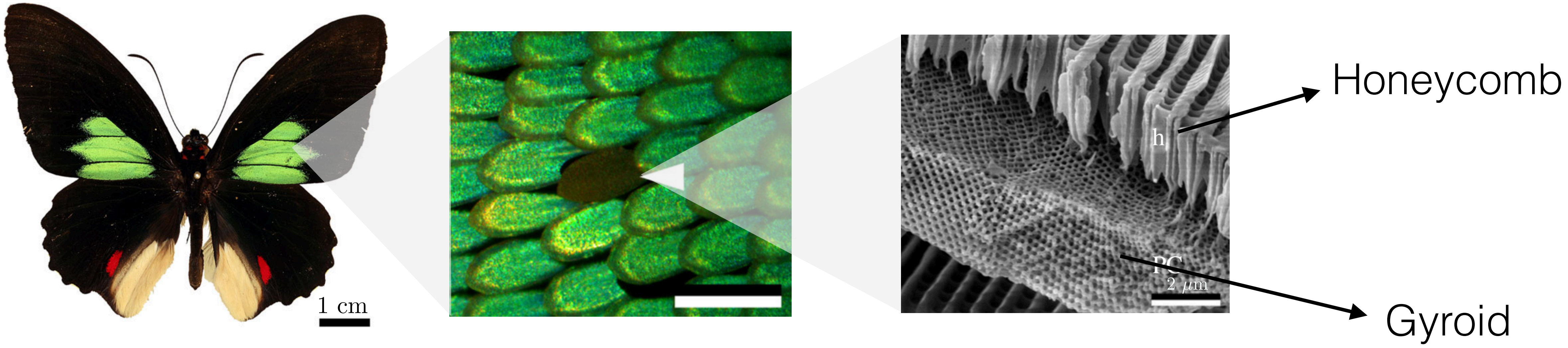

Hales, T. C. (2001). The Honeycomb Conjecture. Discrete & Computational Geometry, 25(1), 1–22.
Dolan et al. (2014). Optical Properties of Gyroid Structured Materials: From Photonic Crystals to Metamaterials. Advanced Optical Materials, 3(1), 12–32.
Wilts, B. D. et al (2012) Iridescence and spectral filtering of the gyroid-type photonic crystals in Parides sesostris wing scales. Interface Focus.

Dispersion diagram of microstructured solid

Dispersion diagram : the fingerprint of a microstructure material

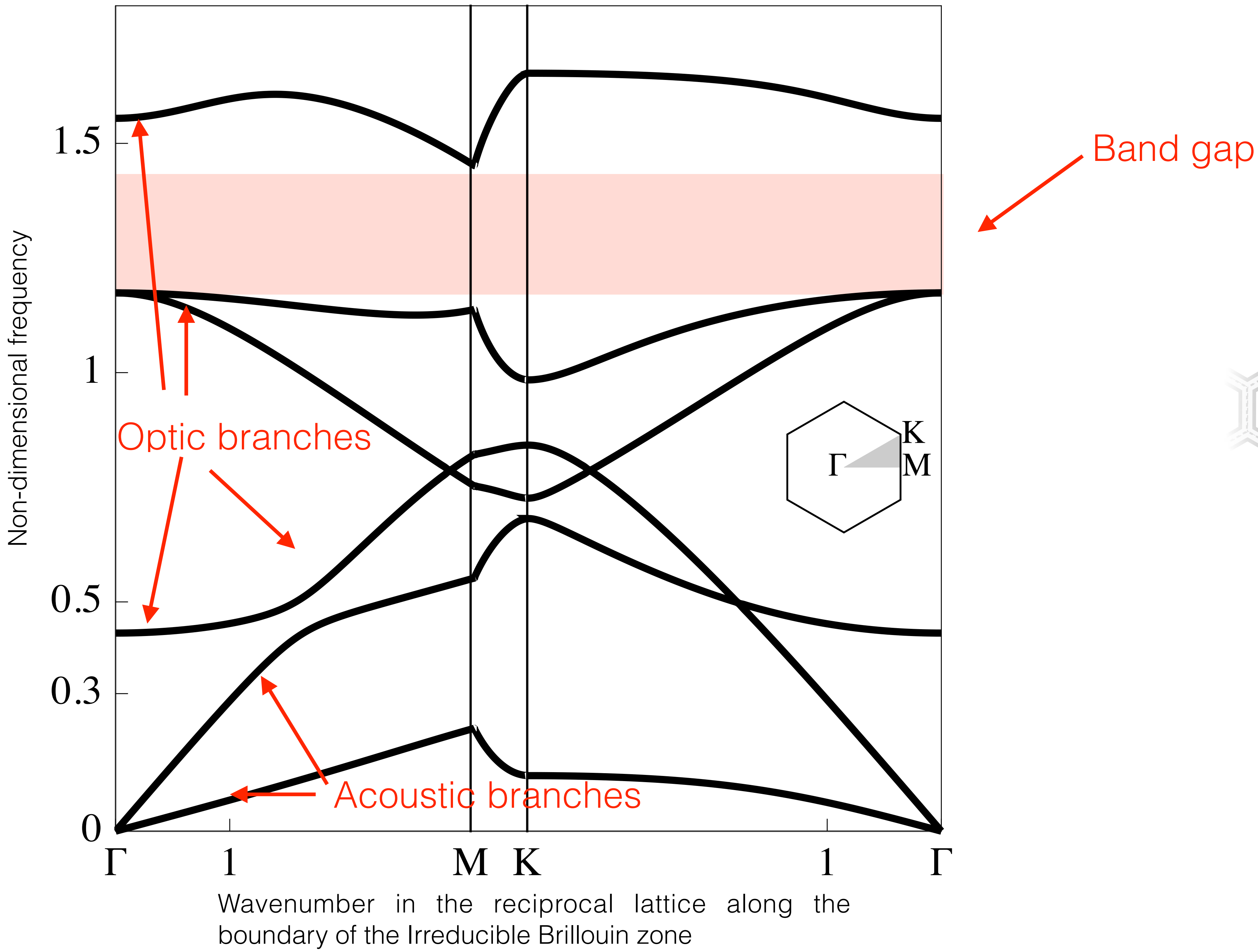

Which generalised continuum model?

Classic continuum:

Very long wavelength approximation

Micromorphic continuum:

Dispersion
Directivity
Optic branches
Band gaps (relaxed micromorphic)

Strain gradient continuum:

Dispersion
Directivity
Decreased number of parameters

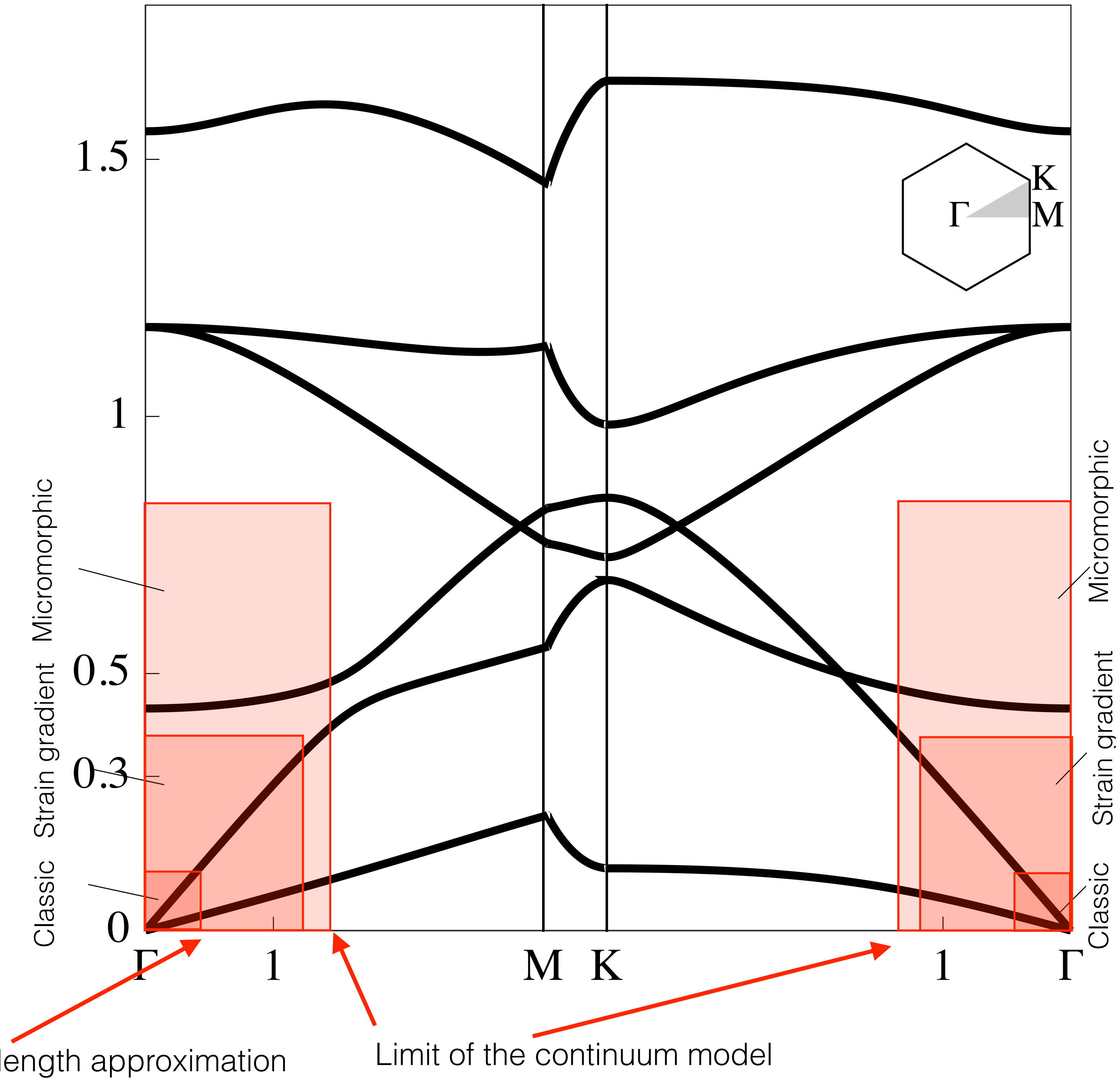

Is there enough information to justify the additional complexity?
What is the size of this domain?

Overview of the strain gradient model

Elastic energy

$$\frac{1}{2}\left(\underset{\sim}{\sigma} : \underset{\sim}{\varepsilon}\right) + \frac{1}{2}\left(\underset{\approx}{\tau} \,\vdots\, \nabla \underset{\sim}{\varepsilon}\right)$$

Strain tensor; Gradient of strain tensor; Stress tensor; Hyper-Stress tensor

Kinetic energy

$$\frac{1}{2}\left(\underline{p} \cdot \underline{\dot{u}}\right) + \frac{1}{2}\left(\underset{\sim}{q} : \nabla \underline{\dot{u}}\right)$$

Velocity; Gradient of velocity; Momentum; Hyper momentum

Balance equation

$$\nabla \cdot \left(\underset{\sim}{\sigma} - \nabla \cdot \underset{\approx}{\tau}\right) = \underline{\dot{p}} - \nabla \cdot \underset{\sim}{\dot{q}}$$

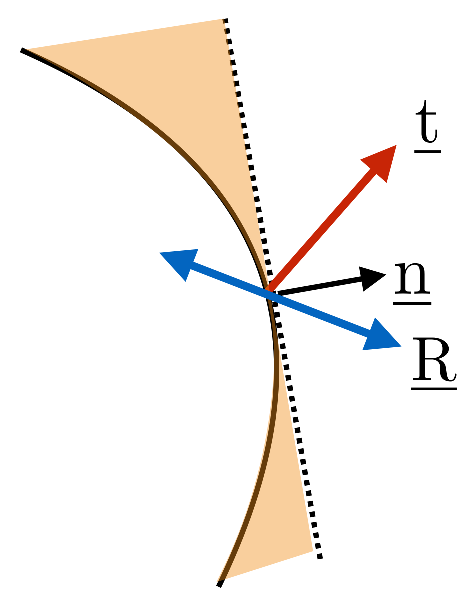

Boundary conditions

Traction

$$\underline{t} = \left(\underset{\sim}{\sigma} - \nabla \cdot \underset{\approx}{\tau} + \underset{\sim}{\dot{q}}\right)\underline{n} + \nabla^S \cdot \left(\underset{\approx}{\tau}\,\underline{n}\right)$$

Hyper traction

$$\underline{R} = \left(\underset{\approx}{\tau}\,\underline{n}\right)\underline{n}$$

Edge (wedge) forces

$$\underline{\nu} = [[\underset{\approx}{\tau}\,\underline{n}_1 \otimes \underline{n}_2]]$$

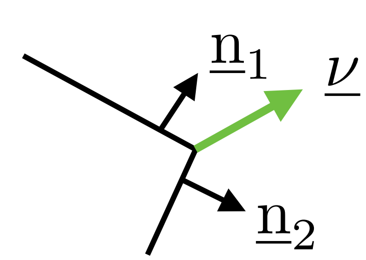

Constitutive equations

The complete set of constitutive equations is

$$
\begin{pmatrix} \underline{\mathrm{p}} \\ \underset{\sim}{\mathrm{q}} \\ \underset{\sim}{\sigma} \\ \underset{\simeq}{\tau} \end{pmatrix}
=
\begin{pmatrix}
\rho \underset{\sim}{\mathrm{I}} & \underset{\simeq}{\mathrm{K}} & 0 & 0 \\
\underset{\simeq}{\mathrm{K}}^T & \underset{\approx}{\mathrm{J}} & 0 & 0 \\
0 & 0 & \underset{\approx}{\mathrm{C}} & \underset{\approxeq}{\mathrm{M}} \\
0 & 0 & \underset{\approxeq}{\mathrm{M}}^T & \underset{\underset{\sim}{\approx}}{\mathrm{A}}
\end{pmatrix}
\begin{pmatrix} \underline{\mathrm{v}} \\ \nabla \underset{\sim}{\mathrm{v}} \\ \underset{\sim}{\varepsilon} \\ \underset{\simeq}{\eta} \end{pmatrix}
$$

$\rho I_{(ij)}$	macroscopic mass density
K_{ijk}	coupling inertia tensor
$J_{\underline{(ij)}\ \underline{(kl)}}$	second order inertia tensor
$C_{\underline{(ij)}\ \underline{(kl)}}$	classical elasticity tensor
$M_{(ij)(lm)n}$	coupling elasticity tensor
$A_{\underline{(ij)k}\ \underline{(lm)n}}$	second order elasticity tensor

N. Auffray et al, "A complete description of bi-dimensional anisotropic strain-gradient elasticity," *Int. J. Solids. Struct.*, 2015.

A new acoustic tensor

Plane wave solution for the displacement

$$u_i = U_i \mathcal{A} \exp\left[\imath\omega\left(t - \frac{1}{V}\hat{\xi}_i x_i\right)\right]$$

Injecting the solution into the balance equation gives

$$\hat{Q}_{il} U_l = \hat{\rho}_{il} V^2 U_l$$

where the **generalised (or effective) acoustic tensor** is

$$\hat{Q}_{il} = C_{ijlm}\hat{\xi}_j\hat{\xi}_m + i\frac{\omega}{V} M^{\sharp}_{ijlmn}\hat{\xi}_j\hat{\xi}_m\hat{\xi}_n + \frac{\omega^2}{V^2} A_{ijklmn}\hat{\xi}_j\hat{\xi}_k\hat{\xi}_m\hat{\xi}_n$$

and the **generalised (or effective) mass** is

$$\hat{\rho}_{il} = \rho\delta_{il} + i\frac{\omega}{V} K^{\sharp}_{ilm}\hat{\xi}_l + \frac{\omega^2}{V^2} J_{ijlm}\hat{\xi}_j\hat{\xi}_m$$

Eigenvectors → Polarization of plane waves

Eigenvalues → Phase velocity of the plane wave

Anisotropic constitutive law

The constitutive law for a D6 material in 2D can be decomposed in the following way

$$\mathbb{A}_{D_6}(\Theta) = \mathbb{A}_{O(2)} + a_D \mathbb{A}_D(6\Theta)$$

Isotropic part, four coefficients

Anisotropic part, one coefficient

Only a combination of the four isotropic coefficients appears in phase and group velocities, so that the coefficients to identify reduce to 3

$$a_S \qquad a_P \qquad a_D$$

The micro inertia tensor is considered isotropic, thus we add two more coefficients

$$\underset{\approx}{J} = \begin{pmatrix} J_P & J_P - 2J_S & 0 \\ J_P - 2J_S & J_P & 0 \\ 0 & 0 & 2J_S \end{pmatrix}$$

Identification

Phase velocities

$\theta = 0^o$

$$v_p(k) = \sqrt{\frac{c_P + (a_P + a_D)k^2}{\rho + J_P k^2}}$$

$$v_s(k) = \sqrt{\frac{c_S + a_S k^2}{\rho + J_S k^2}}$$

$\theta = 30^o$

$$v_p(k) = \sqrt{\frac{c_P + a_P k^2}{\rho + J_P k^2}}$$

$$v_s(k) = \sqrt{\frac{c_S + (a_S + a_D)k^2}{\rho + J_S k^2}}$$

The following values for the parameters are identified by fitting guided wave propagation

c_P	1.25	GPa
c_S	67.4	MPa
ρ	380	$\mathrm{kg/m}^3$
a_P	0.93	$\mathrm{Pa \cdot m}^2$
a_S	0.75	$\mathrm{Pa \cdot m}^2$
a_D	12.5	$\mathrm{Pa\ m}^2$
J_P	5.4×10^{-7}	kg/m
J_S	6×10^{-5}	kg/m

Characteristic length 0.44 mm

The case of hexagonal lattices

Low frequency

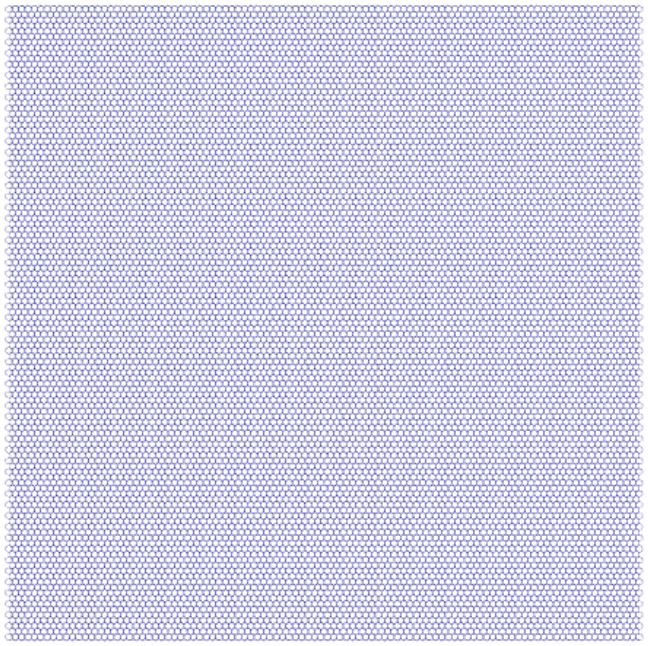

Lattice

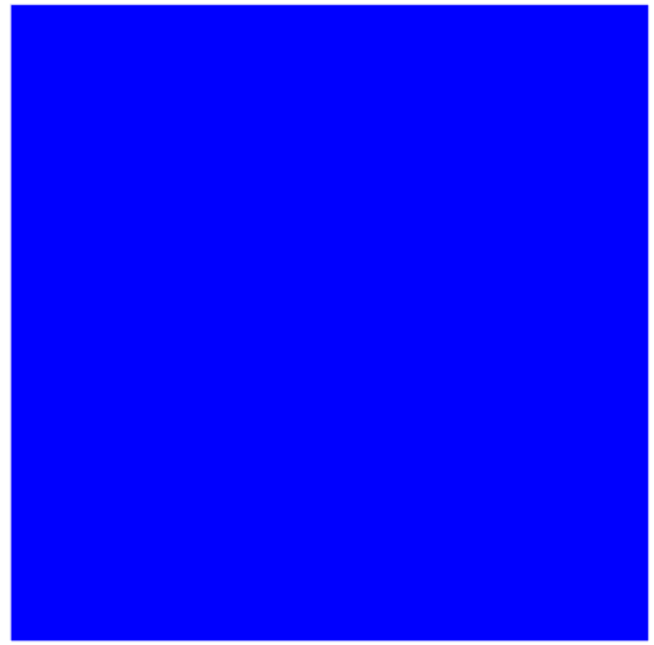

Classic elasticity

Strain gradient

High frequency

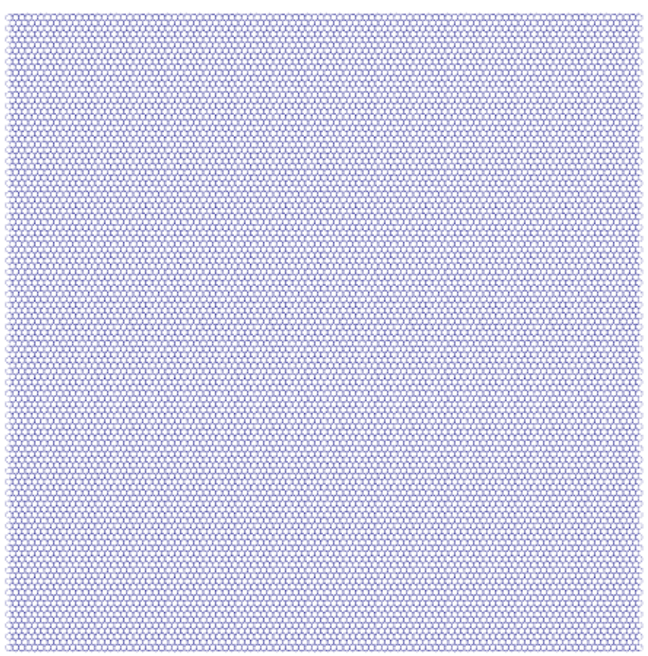

Lattice

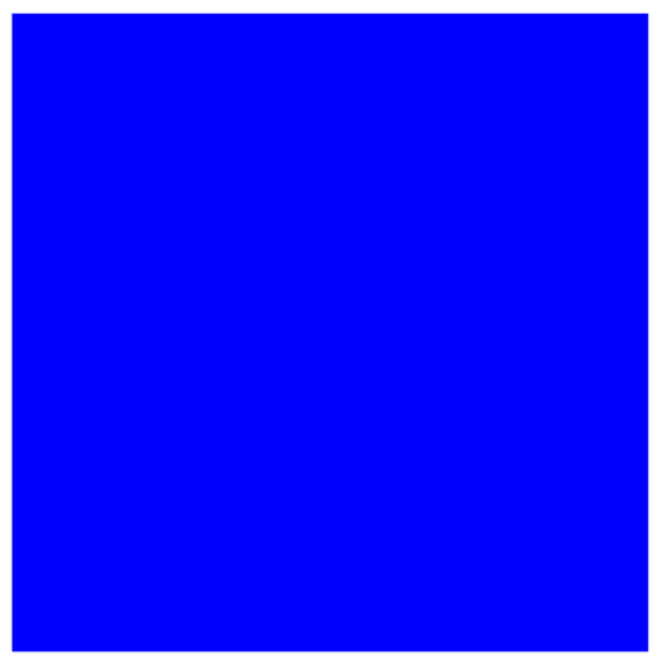

Classic elasticity

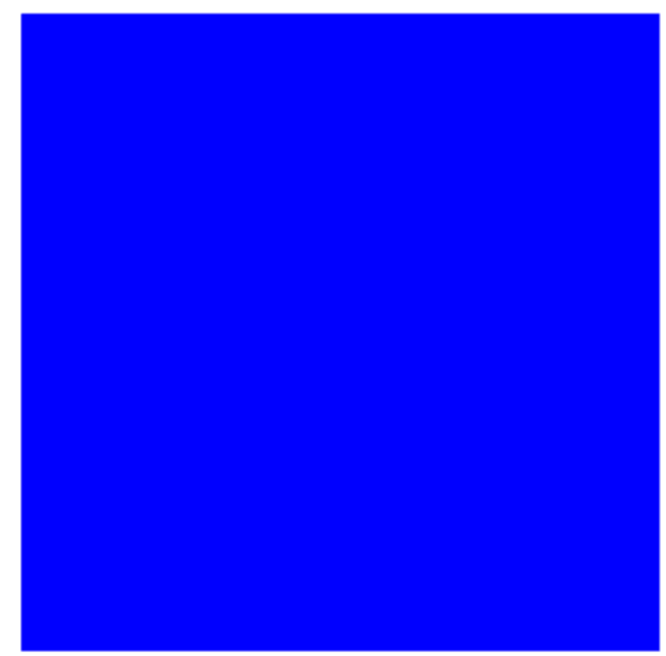

Strain gradient

The gyroid microstructure

Triply periodic minimal surface, known as Shoen's gyroid. Has a simple equation, that can be used to define a volume

Two parameters a, b control respectively the size of the unit cell and the porosity

The equation is the following

$$\sin(a\pi x)\cos(a\pi y) + \cos(a\pi x)\sin(a\pi z) + \sin(a\pi y)\cos(a\pi z) = b$$

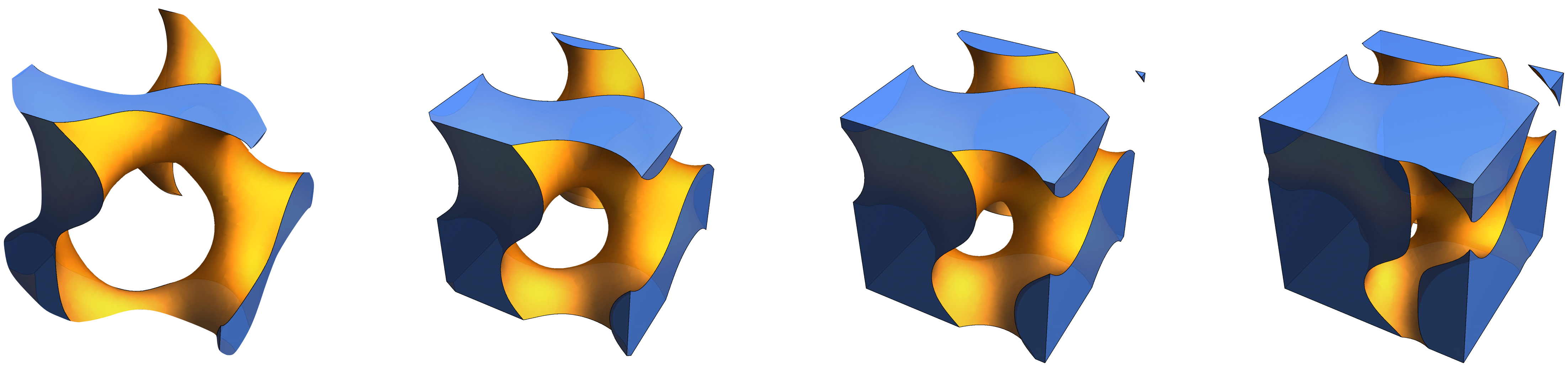

20% 30% 70% 80%

The point group is cubic. The space group is body centred cubic ($I4_132$).

Symmetries

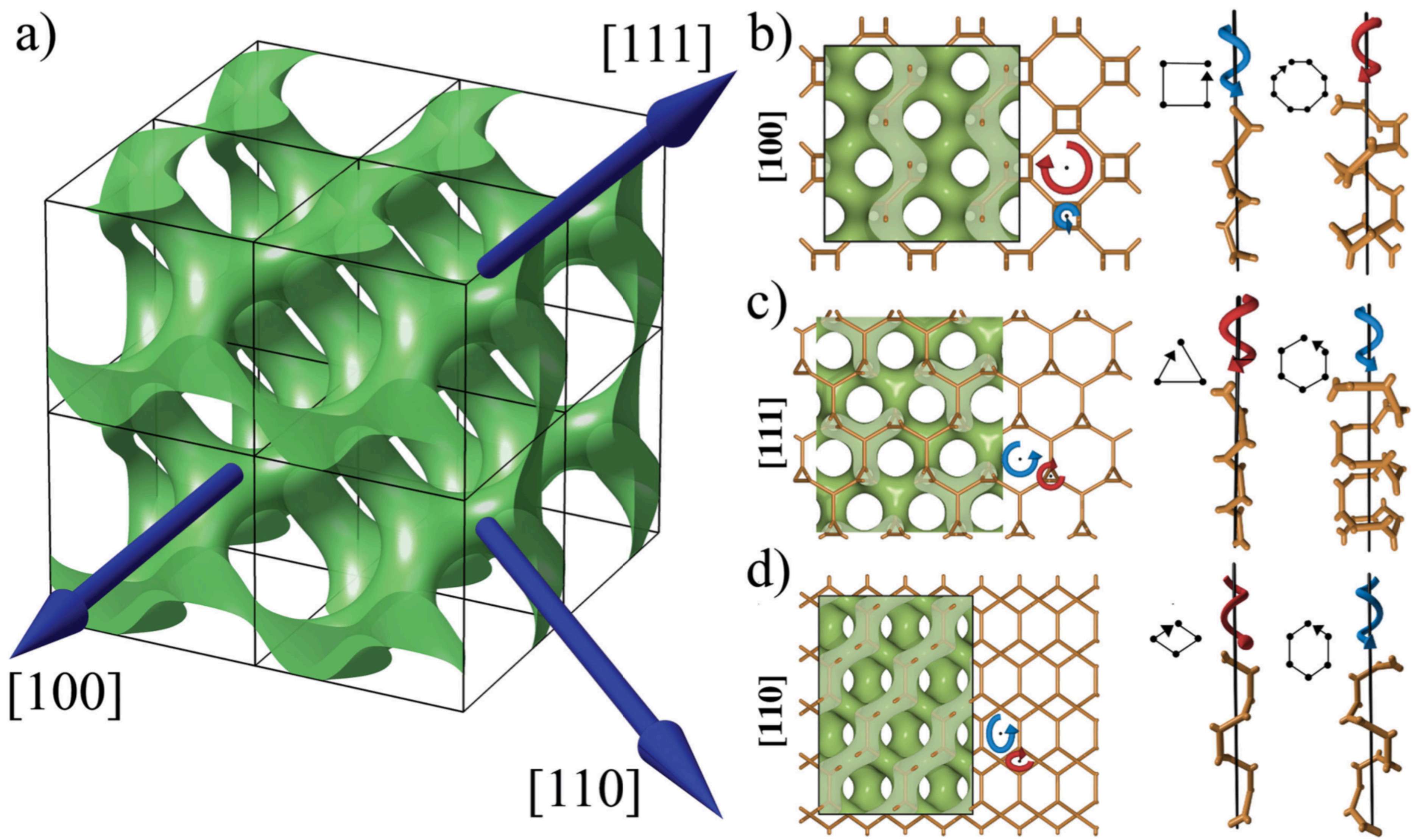

Interesting symmetries can be observed on the planes orthogonal to major symmetry axes

Dolan, J. A. et al (2014). Optical Properties of Gyroid Structured Materials: From Photonic Crystals to Metamaterials. Advanced Optical Materials, 3(1), 12–32

Dispersion diagram

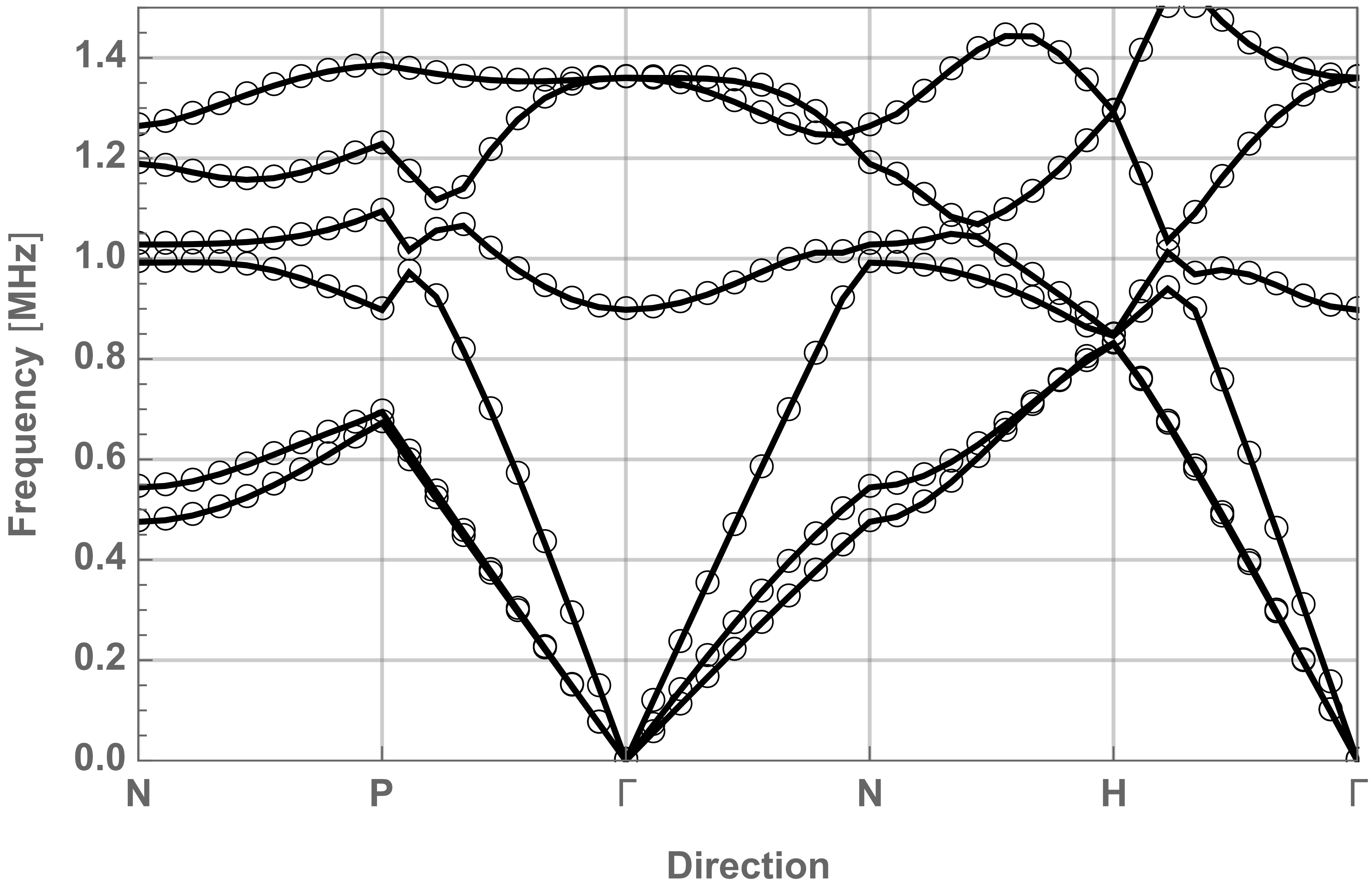

Dispersion diagram for a Gyroid made of Titanium and porosity 0.7

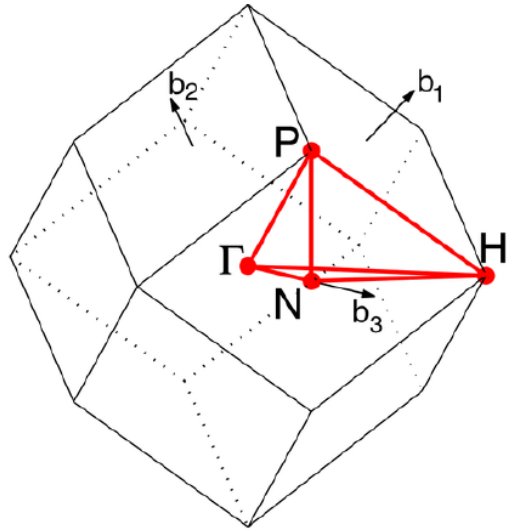

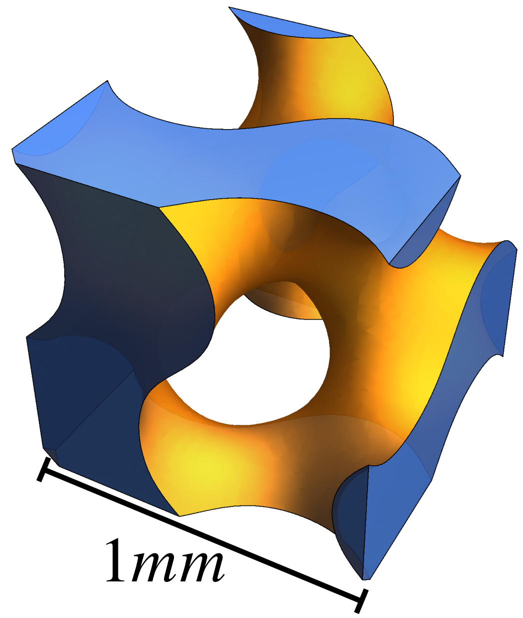

Elasticity vs optics

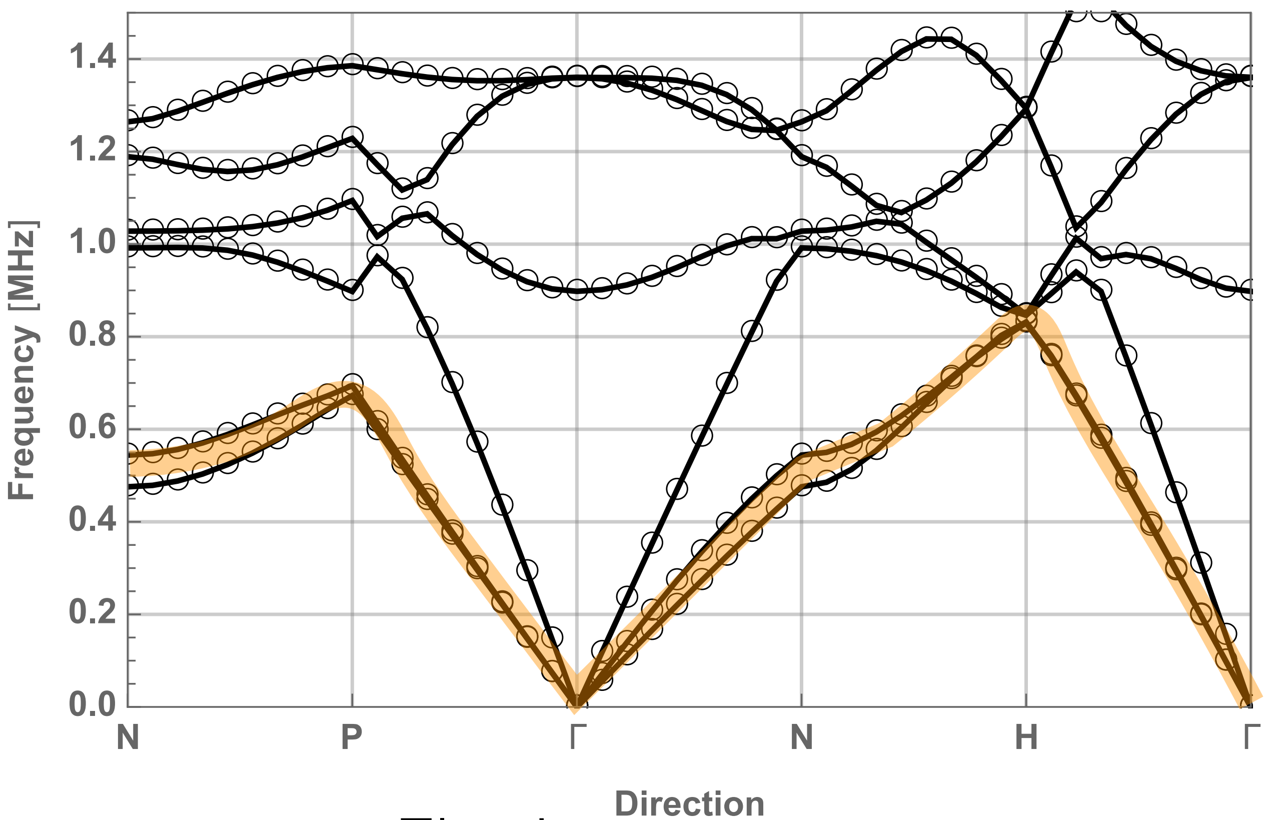

Elastic waves

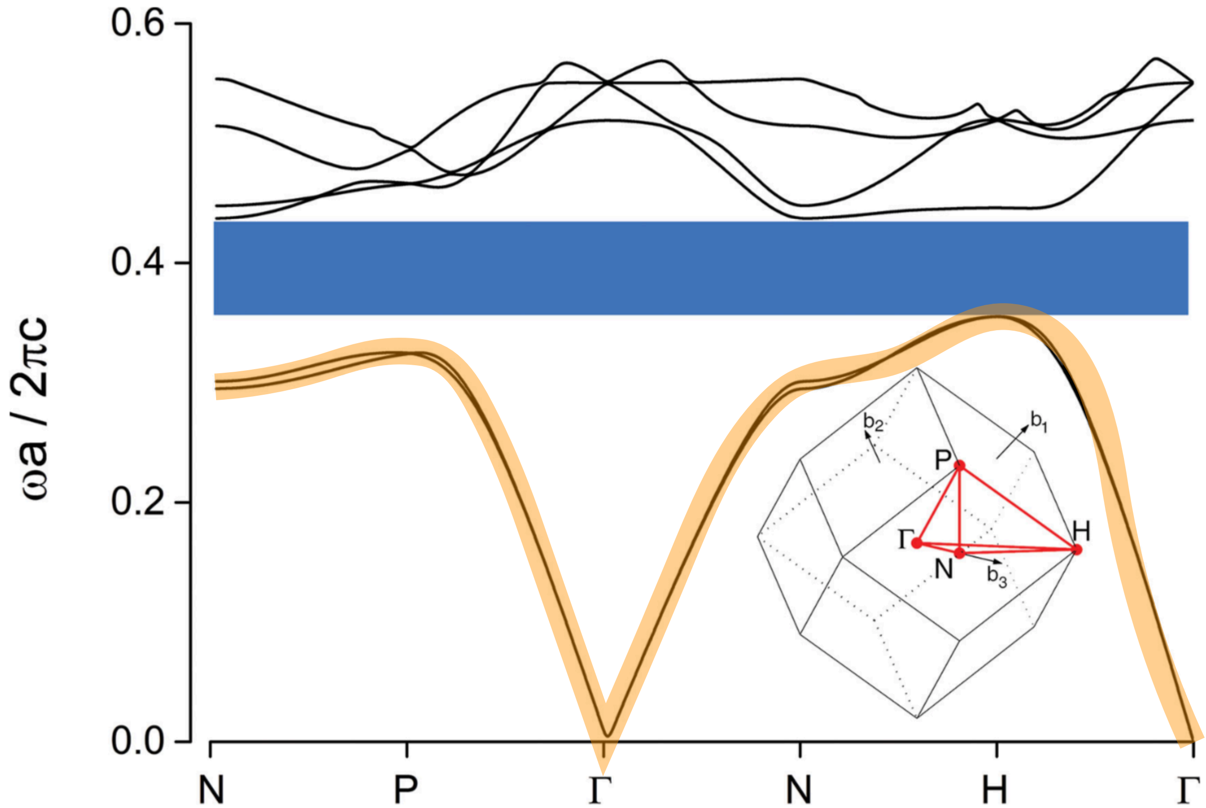

Electromagnetic waves

Circular polarisation observed in directions ΓH ([100]) and ΓP ([111])

Optical dicrhoism is observed for these waves, optical devices are built on this principle (e.g. beam splitters)

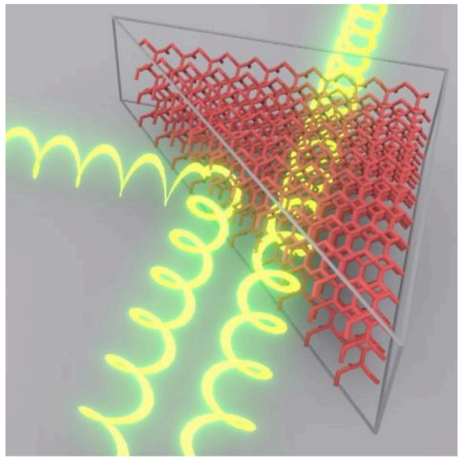

Polarisation of waves

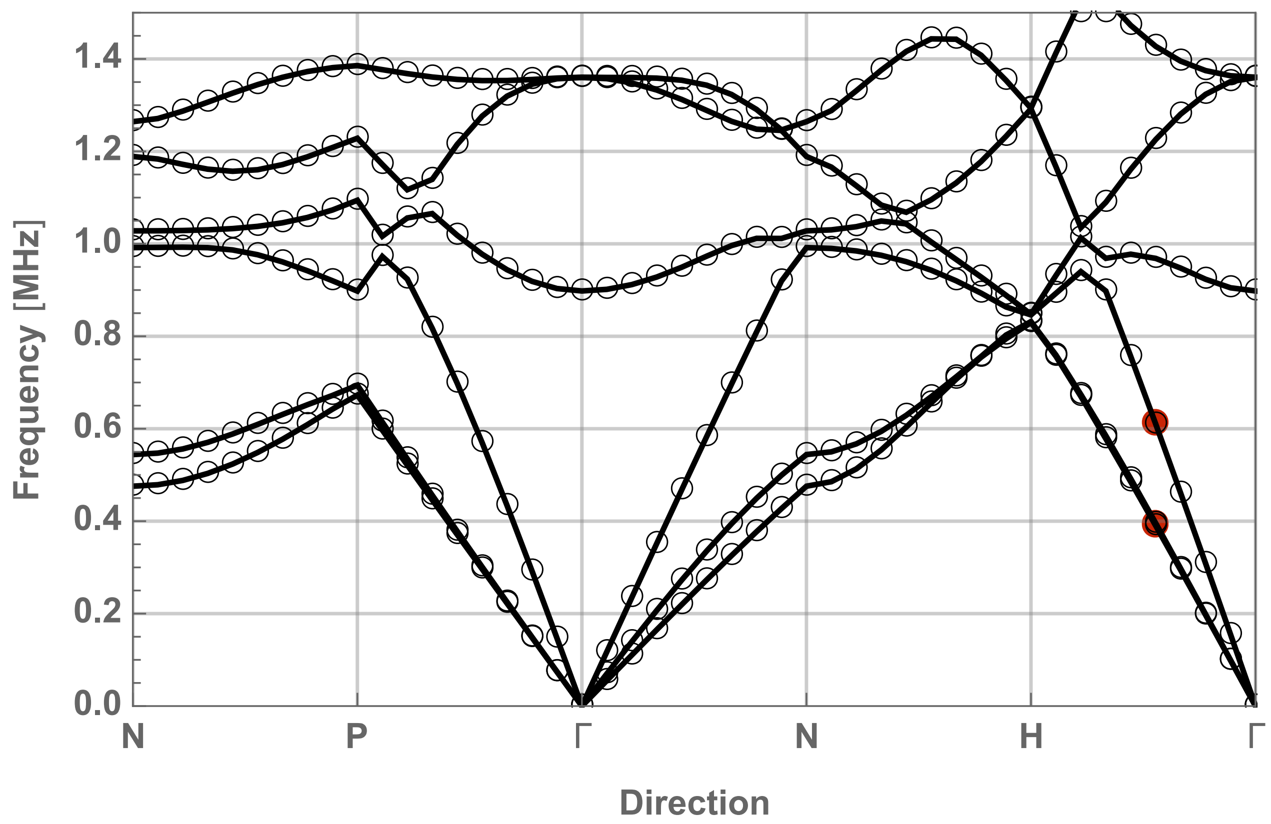

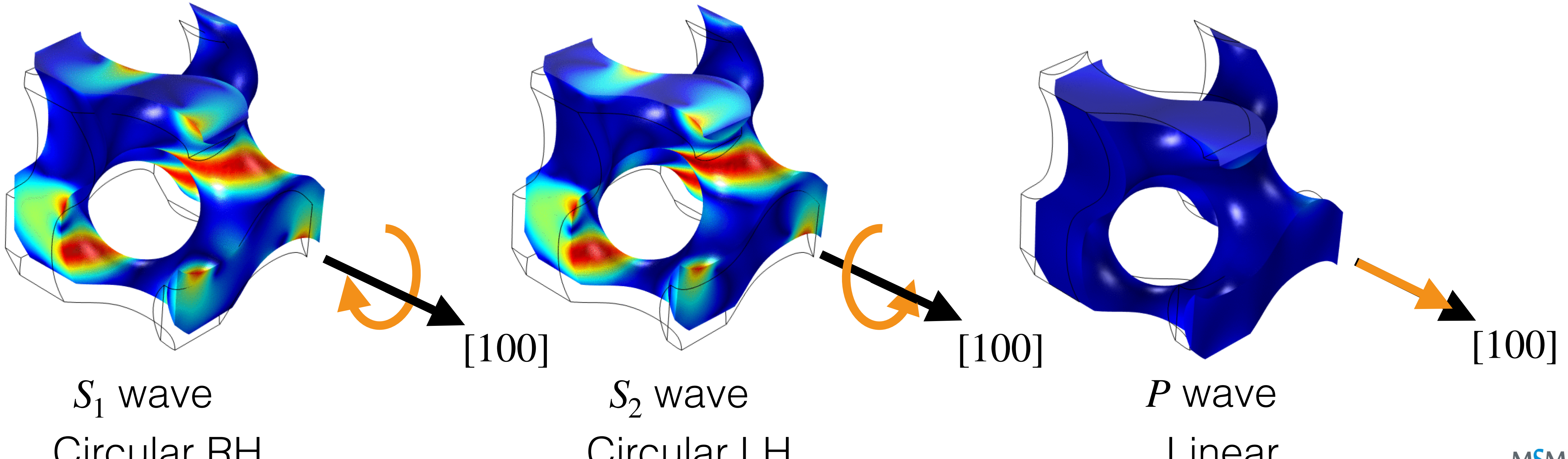

Constitutive equations

$$\begin{pmatrix} \underline{\mathrm{p}} \\ \underset{\sim}{\mathrm{q}} \\ \underset{\sim}{\sigma} \\ \underset{\approx}{\tau} \end{pmatrix} = \begin{pmatrix} \rho \underset{\sim}{\mathrm{I}} & \underset{\approx}{\mathrm{K}} & 0 & 0 \\ \underset{\approx}{\mathrm{K}}^T & \underset{\approx}{\mathrm{J}} & 0 & 0 \\ 0 & 0 & \underset{\approx}{\mathrm{C}} & \underset{\approx}{\mathrm{M}} \\ 0 & 0 & \underset{\approx}{\mathrm{M}}^T & \underset{\approx}{\mathrm{A}} \end{pmatrix} \begin{pmatrix} \underline{\mathrm{v}} \\ \underset{\sim}{\nabla \mathrm{v}} \\ \underset{\sim}{\varepsilon} \\ \underset{\approx}{\eta} \end{pmatrix}$$

macroscopic mass density	$\rho I_{(ij)}$	1
coupling inertia tensor	$K^{\sharp}_{\underline{ij}k}$	1
second order inertia tensor	$J_{\underline{(ij)}\,\underline{(kl)}}$	3
classical elasticity tensor	$C_{\underline{(ij)}\,\underline{(kl)}}$	3
coupling elasticity tensor	$M^{\sharp}_{\underline{(ij)}\overline{(lm)}n}$	2
second order elasticity tensor	$A_{\underline{(ij)k}\,\underline{(lm)n}}$	11
		21

Auffray, N.et al. (2013). Matrix representations for 3D strain-gradient elasticity. *Journal of the Mechanics and Physics of Solids*, *61*(5), 1202–1223.
Auffray, N. et al. Complete symmetry classification and compact matrix representations for 3D strain gradient elasticity. To be submitted

Phase velocities and polarisations

$$
\begin{pmatrix} \underline{\mathrm{p}} \\ \underset{\sim}{\mathrm{q}} \\ \underset{\sim}{\sigma} \\ \underset{\approx}{\tau} \end{pmatrix} = \begin{pmatrix} \rho \underset{\sim}{\mathrm{I}} & \underset{\approx}{\mathrm{K}} & 0 & 0 \\ \underset{\approx}{\mathrm{K}}^T & \underset{\approx}{\mathrm{J}} & 0 & 0 \\ 0 & 0 & \underset{\approx}{\mathrm{C}} & \underset{\approx}{\mathrm{M}} \\ 0 & 0 & \underset{\approx}{\mathrm{M}}^T & \underset{\underset{\sim}{\approx}}{\mathrm{A}} \end{pmatrix} \begin{pmatrix} \underline{\mathrm{v}} \\ \underset{\sim}{\nabla \mathrm{v}} \\ \underset{\sim}{\varepsilon} \\ \underset{\approx}{\eta} \end{pmatrix}
$$

The generalised Christoffel equation for the direction $\underline{n} = (1,0,0)$ gives the following phase velocities

$$v_1 = \sqrt{\frac{c_{44} - km_1 + k^2 a_{S_1}}{\rho - kK + k^2 j_{S_1}}} \qquad v_2 = \sqrt{\frac{c_{44} + km_1 + k^2 a_{S_1}}{\rho + kK + k^2 j_{S_1}}} \qquad v_3 = \sqrt{\frac{c_{11} + k^2 a_P}{\rho + k^2 j_P}}$$

and complex polarisations

$\underline{u}_1 = (0, -i, 1)$ — Circular RH

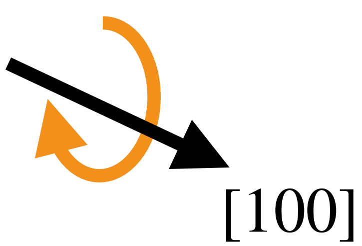

$\underline{u}_1 \cdot \underline{u}_1 = 0$

$\left[\underline{u}_2^R \; \underline{u}_2^I \; \underline{n}\right] > 0$

$\underline{u}_2 = (0, i, 1)$ — Circular LH

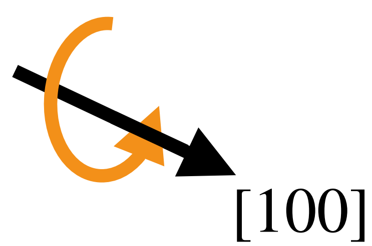

$\underline{u}_2 \cdot \underline{u}_2 = 0$

$\left[\underline{u}_2^R \; \underline{u}_2^I \; \underline{n}\right] < 0$

$\underline{u}_3 = (0, 0, 1)$ — Linear

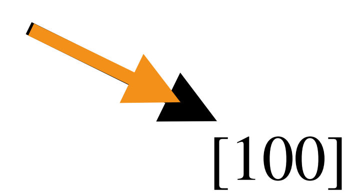

$\underline{u}_3^R \times \underline{u}_3^I = \underline{0}$

Circular polarisation

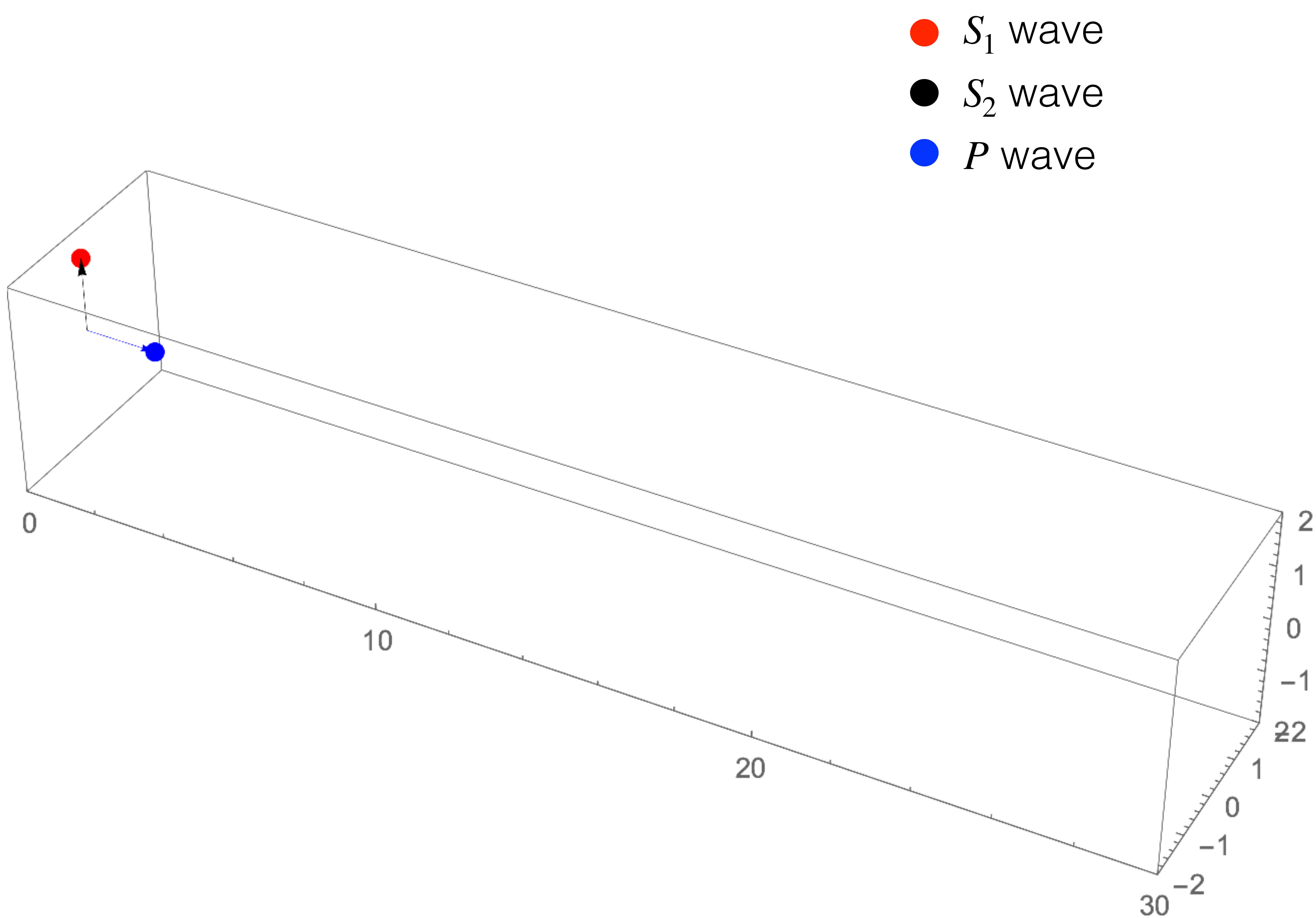

Conclusions and perspectives

Main results

- Generalised continua are an effective tool to study wave propagation in microstructured material
- The choice of the model and its domain of validity depends on the problem
- Results from metamaterials can be of use in biomechanics

Perspectives in tissue engineering

- Optimisation of ultrasonic properties (tailored ultrasonic signature)
- Enhanced osteointegration monitoring
- Real time quality assessment of the microstructure (phononic properties)

Things to do next

- Experimental validation (in progress)
- Reliable procedure for the estimation of the coefficients (based on guided propagation)

References

[1] N. Auffray, J. Dirrenberger, and G. Rosi, “A complete description of bi-dimensional anisotropic strain-gradient elasticity,” Int. J. Solids. Struct., vol. 69, pp. 195–206, 2015.

[2] G. Rosi and N. Auffray, “Anisotropic and dispersive wave propagation within strain-gradient framework,” Wave Motion, vol. 63, pp. 120–134, 2016.

[3] G. Rosi, L. Placidi, and N. Auffray, “On the validity range of strain-gradient elasticity: A mixed static-dynamic identification procedure,” Eur. J. Mech. A-Solids, vol. 69, pp. 179–191, 2018.

[4] G. Rosi and N. Auffray, “Continuum modelling of frequency dependent acoustic beam focusing and steering in hexagonal lattices”, Eur. J. Mech. A-Solids, 2019